



# Analysis of ionospheric TEC anomalies for global earthquakes during 2000-2019 with respect to earthquake magnitude ( $M_w \geq 6.0$ )

Mustafa Ulukavak<sup>a,\*</sup>, Mualla Yalçinkaya<sup>b</sup>, Emine Tanır Kayıkcı<sup>b</sup>, Serkan Öztürk<sup>c</sup>, Raif Kandemir<sup>d</sup>, Hakan Karslı<sup>e</sup>

<sup>a</sup> Harran University, Engineering Faculty, Department of Geomatic Engineering, Sanlıurfa, Turkey

<sup>b</sup> Karadeniz Technical University, Engineering Faculty, Department of Geomatic Engineering, Trabzon, Turkey

<sup>c</sup> Gümüşhane University, Faculty of Engineering and Natural Sciences, Department of Geophysics, Gümüşhane, Turkey

<sup>d</sup> Recep Tayyip Erdoğan University, Engineering Faculty, Department of Geology Engineering, Rize, Turkey

<sup>e</sup> Karadeniz Technical University, Engineering Faculty, Department of Geophysics, Trabzon, Turkey

## ARTICLE INFO

### Keywords:

Ionospheric total electron content (TEC)  
Earthquake magnitude  
Geomagnetic storm indices  
Solar activity indices

## ABSTRACT

In this work, a relationship between ionospheric TEC anomalies and different earthquake magnitude groups before the main shocks was investigated. For this purpose, 2942 global earthquakes with  $M_w \geq 6$  from 2000 to 2019 and possible ionospheric TEC anomalies that occurred before earthquakes were examined by considering 13 different index values of space weather conditions (geomagnetic storm indices and solar activity indices). Anomalies of ionospheric TEC changes were defined for 15-days before and 4-days after the earthquakes by using 15-days moving median method with the length of 15 days. Earthquakes were first grouped according to their magnitudes, and then negative and positive TEC anomalies in quiet days before the earthquakes were detected. These anomalies were observed as  $\sim 5-13$ ,  $\sim 5-10$ ,  $\sim 5-15$ ,  $\sim 3-13$ ,  $\sim 7-15$ ,  $\sim 1$  and  $\sim 5-8$  days ago for the earthquakes of  $6.0 \leq M_w < 6.5$ ,  $6.5 \leq M_w < 7.0$ ,  $7.0 \leq M_w < 7.5$ ,  $7.5 \leq M_w < 8.0$ ,  $8.0 \leq M_w < 8.5$ ,  $8.5 \leq M_w < 9.0$ , and  $9.0 \leq M_w < 9.5$ , respectively. Mean of changes in TEC anomalies of these groups is 44.2 % TECU and we detected that the number of positive anomalies in each group is larger than the number of negative anomalies. Consequently, these analyses clearly show that the day-to-day changes in TEC anomalies may supply significant precursors prior to the global earthquakes ( $M \geq 6$ ) in the short-term earthquake prediction for main shocks.

## 1. Introduction

Earthquake prediction has been a very complex and important issue in seismology for more than a century. The phrase of “*short term prediction*” states the alarms from days to months, “*intermediate term prediction*” from a few months to several years, and “*long term prediction*” from a few years to several decades. Current progress in literature reveals that acceptable and reliable models in earthquake prediction have not yet been available in the short-term in comparison with the intermediate or long term. That means the effective short term prediction is still a challenging issue (Sykes, 2002). The phrase of “*short term prediction*” states the alarms from days to months, “*intermediate term prediction*” from a few months to several years, and “*long term prediction*” from a few years to several decades. However, the short-term earthquake prediction has a critical review and it may be difficult to detect the potential precursory anomalies for the short-term earthquake

hazard (Huang et al., 2017). Thus, successful earthquake predictions in the short term for the near future earthquakes have been uncommon on a reliable and consistent basis.

It is well known that earthquakes do not occur randomly in space and time. Aftershocks, foreshocks, groundwater level and temperature, changes in animal behaviours, electromagnetic signals, precursory fault slip, chemical emissions, temporal variations of velocity, precursory quiescence or seismic activation are just a few of the indicators identified by seismologists (Holliday et al., 2005). In addition, many well-accepted seismological, geodetic and other geophysical precursors such as geomagnetic, geoelectric, geodetic and gravity precursors, ground fluid or hydro-seismology can be observed and monitored to develop the earthquake prediction practice (Geller, 2007; Huang et al., 2017). Since earth's crust is highly complex and earthquakes are generally to be chaotic, earthquake predictions can be thought on a statistical basis and these statistical behaviours of earthquake occurrences can be

\* Corresponding author.

E-mail address: [mulukavak@harran.edu.tr](mailto:mulukavak@harran.edu.tr) (M. Ulukavak).

utilized to predict the next possible earthquakes (Rundle et al., 2003). Therefore, the main problem in the earthquake prediction studies is whether or not the statistical properties of earthquake occurrences can be used to predict future earthquakes. There are many different algorithms used for the earthquake prediction. However, these models have generally two approaches: the first group approaches are based on the empirical measurements of precursory seismicity changes whereas the second is based on the statistical models of earthquake activity. For this purpose, many researchers have made earthquake predictions for different regions of the world by developing different approaches such as VAN method (Varotsos and Alexopoulos, 1984), Region-Time-Length (RTL) algorithm (Huang et al., 2001; Sobolev and Tyupkin, 1997), ZMAP technique (Wiemer, 2011), M8 and CN algorithms (Shcherbakov, 2003), PI and RI techniques (Nanjo et al., 2006; Tiampo et al., 2002). Although these approaches have some advantages or disadvantages compared to each other, and the best method does not exist. All the above mentioned methods allow users to measure, map and evaluate the possible earthquake hazard in the intermediate and long term for different seismicity regions of the world.

Since the 1900s, earthquake prediction studies have successfully been made and some of them are given here. For example, a successful prediction for February 4, 1975 ( $M_s=7.3$ ) earthquake was based on foreshocks and other geophysical parameters (Huang et al., 2017). Also, a successful prediction of the earthquake location was made for October 23, 2004, Niigata, Japan ( $M = 6.8$ ) earthquake. As a global long-term forecast, the locations of December 23, 2004 ( $M = 8.1$ ) Macquarie Island earthquake and of December 26, 2004 ( $M = 9.0$ ) Sumatra earthquake were predicted successfully (Holliday et al., 2005). Öztürk (2011) made a statistical evaluation to detect the precursory seismic quiescence in and around the North Anatolian Fault Zone in Turkey and published successful prediction for future earthquakes such as September 22, 2011 ( $M = 5.6$ ) Refahiye-Erzincan, July 30, 2013 ( $M = 5.3$ ) Gökçeada-Çanakkale and December 3, 2015 Kığı-Bingöl ( $M = 5.5$ ) earthquakes. It is clear that these examples of predictions include the intermediate or long terms evaluations of future earthquakes. However, examples of successful short-term predictions for the next earthquakes have been uncommon and short-term predictions may provide a successful probabilistic hazard assessment for earthquake risk.

The main goal of this study is to present a novel methodology of the short-term earthquake prediction and to make a contribution to an effective prediction for large/destructive earthquakes. Although earthquake catalogues as the complete and long observations including about 50–100 years are generally used for the prediction, some environmental changes mentioned above can provide significant signs before the occurrences of earthquakes. One of the most encouraging methods among these precursory chances can be given as the monitoring ionospheric Total Electron Content (TEC) variations in TEC unit ( $1 \text{ TECU} = 10^{16} \text{ electron/m}^2$ ). In recent years, a lot of research has been done on this subject (Table 1). In our statistical-based novel method, we have included variables belongs to environmental changes, the electromagnetic emissions from ground in a wide signal spectrum, atmospheric and ionospheric events and local magnetic field changes, fluctuations in the ionospheric TEC anomalies for the short-term earthquake prediction. Thus, this study will provide preliminary and remarkable information about such an effort by supplying a new perspective.

## 2. Data and methods

In this research, 2942 earthquakes with  $M_w \geq 6.0$  occurred in different regions of the world between 2000 and 2019 freely available in the earthquake database and fault catalogues in the USGS earthquakes web interface were obtained (<http://earthquake.usgs.gov/earthquakes/search/>) (Fig. 1). The classification of earthquakes according to their magnitude and the number of earthquakes in each group were given in Table 2. Table 2 shows that 69 %, 30 % and 1% of total earthquakes

have occurred between  $6.0 \leq M_w < 6.5$ ,  $6.5 \leq M_w < 8.0$  and  $8.0 \leq M_w < 9.5$ , respectively. All maps, graphics, calculations and some statistical procedures were performed in MATLAB® (2017b) environment.

### 2.1. The relation between earthquakes and ionospheric anomalies

It is quite difficult to define directly the environmental structure of the preparatory stage occurred prior to the earthquakes and therefore, it is more accurate to describe the potential effects indirectly by observing the environmental variations. Conversely, these changes might be due to geological, geophysical or atmospheric circumstances, but earthquake occurrences and the effects that trigger these variations have not yet been exactly described (Fidani, 2010; Guo and Wang, 2008; Pulnits et al., 2006; Tronin et al., 2004). During large events, the crust of the earth sometimes shows strong emissions, frequently weak, and it has occasionally short lifespan. Signals includes electromagnetic emissions over a wide frequency range, ionospheric or atmospheric events, regional variations in magnetic field. The peroxy bonds are broken and then electrically charged carriers are released in order to compose positive holes. Positive holes can carry free volumes from trapped volumes without difficulty and they are very mobile. The electric current generated by the positive current transition produces low-frequency electromagnetic radiation and magnetic field changes in a system which works like a battery. Positive holes arrive the earth and then, ionized molecules actualizes between the ground and air interface. Rising and ionizing air can be seen as a potential reason of irregularities in the ionosphere (Freund, 2011; Ulukavak and Yalçinkaya, 2017b). The relationship between earthquake activity and electron density changes has not still been fully figured out today (Namgaladze et al., 2009; Pulnits, 1998). The first theory is related to the electron emission, i.e. piezoelectric effect that is due to the trapped rocks. In a laboratory environment, the upper surface of the granite block was exposed to the pressure and then, ionization of the molecules was shown in the air contacted side of the granite block (Freund et al., 2009). Electrons ( $e^-$ ) and the positively charged carrier holes ( $h^+$ ) flow through the pressured rock volume to the non-pressured side of the granite and then a current occurs between the pressure applied side and end of the rock block. This difference behaves as an current over the battery. The pressed side acts as a negative pole of the battery cell and is also loaded with positively charged molecules. The charge carrier  $h^+$  allows the positive holes to be held on the surface. The proven and confined Rocks-Earth surface variations in the lithosphere-atmosphere-ionosphere system will be formed by the spatial expansion of this experiment and this system cause the ionization in the rocks with the stress accumulated in the fault ruptures before the strong events. Also, this system spreads the ionized air to the ionosphere layer and increase the electron density in the ionosphere (Kuo et al., 2011; St-Laurent et al., 2006; Ulukavak and Yalçinkaya, 2017b). By considering this theory, earthquakes were classified according to their magnitudes with ionospheric TEC anomalies.

Positive and negative ionospheric anomalies occur before earthquakes. It is considered that positive ionospheric anomalies are caused by the increase of electron oscillations in the ionosphere due to the p-holes whereas negative ionospheric anomalies arise from mostly in the Sub-Ionospheric Points (SIP) far away from earthquake epicentre (Heki, 2011). These negative anomalies return to normal again by disappearing together with Co-seismic Ionospheric Disturbances (CID) emerged with earthquakes.

From previous studies in the literature, it has been revealed that earthquakes which occurred land and oceanic regions cause ionospheric TEC anomalies in advance earthquake (He and Heki, 2017; Sunardi et al., 2018; Tao et al., 2017; Xia et al., 2011; Zhu et al., 2018). Li and Parrot (2013) showed that the earthquakes occurred under the oceans provide more anomalies than those of earthquakes occurred on lands by analysing the ion density changes received from DEMETER

**Table 1**  
Literature studies for the detection of seismo-ionospheric TEC anomalies.

No	Years	Number of EQ	Magnitude of EQ	Space Weather Conditions	Depth of EQ (km)	EQ Precursor (Day)	Reference
1	1999-2002	20	$M \geq 6$	-	-	~1-5	Liu et al. (2004)
2	1994-1999	184	$M \geq 5$	-	-	~5	Liu et al. (2006)
3	1999-2006	5	$M \geq 6$	Kp	-	~1-6	Afraimovich and Astafyeva (2008)
4	1998-2008	17	$M \geq 6$	Dst	-	~3-5	Liu et al. (2009)
5	2008	1	$M = 8$	Dst, Kp F10.7, AE	-	~5-13	Jhuang et al. (2010)
6	2004-2008	4	$M > 6$	Dst	-	~3-6	Liu et al. (2011)
7	1998-2010	52	$M \geq 6$	Dst, Kp F10.7	$\leq 40$	~1-5	Kon et al. (2011)
8	2010	7	$M \geq 7$	Dst, Kp F10.7	-	~8-11	Yao et al. (2012)
9	2002-2010	736	$M \geq 6$	Dst	$\leq 40$	~1-21	Le et al. (2011)
10	2007-2009	50	$M \geq 7$	Kp	$\geq 20$	~10	Fuying et al. (2011)
11	2008-2012	3	$M \geq 7$	Dst, Kp F10.7	$\leq 30$	~5-6	Zhu et al. (2013a)
12	2003-2012	144	$M \geq 7$	Dst	-	~4-7	Zhu et al. (2014)
13	1998-2012	-	$M \geq 6$	-	$\leq 40$	~1-5	Hattori et al. (2014)
14	1998-2014	1492	$M \geq 5$	Dst, Kp F10.7	$\leq 150$	~5	Shah and Jin (2015)
15	2010	2	$M \geq 6$	Dst, Kp EUV 01-50 Bz, Ey	-	~3-4	Aggarwal (2015)
16	2010	1	$M > 7$	Dst, Kp F10.7	-	~1-5	Ulukavak and Yalcinkaya (2017a)
17	2003-2014	133	$M \geq 7$	Dst, Kp F10.7	$\leq 60$	~1-6	Zhu et al. (2016)
18	2000-2014	1279	$M \geq 6$	Kp, Dst	$\leq 40$	X	Thomas et al. (2017)
19	2006-2015	100	$M \geq 7$	Dst, Kp F10.7	-	~8	Li et al. (2018)
20	2003-2016	63	$M \geq 5$	Dst, Kp F10.7	-	~0-10	Şentürk and Çepni (2018)
21	2003-2014	1339	$M \geq 6$	Dst	$\leq 60$	~1-5	Zhu et al. (2018)
22	2015-2017	3	$M \geq 7$	Dst, Kp F10.7, AE	-	~10	Tariq et al. (2019)

satellite.

On the other hand, it has been considered that ionospheric anomalies before the earthquakes happen with different physical

mechanism according to earthquake occurrences on land and under the oceans. This physical mechanism by which possible earthquake-induced ionospheric TEC anomalies on lands occur with p-holes can be

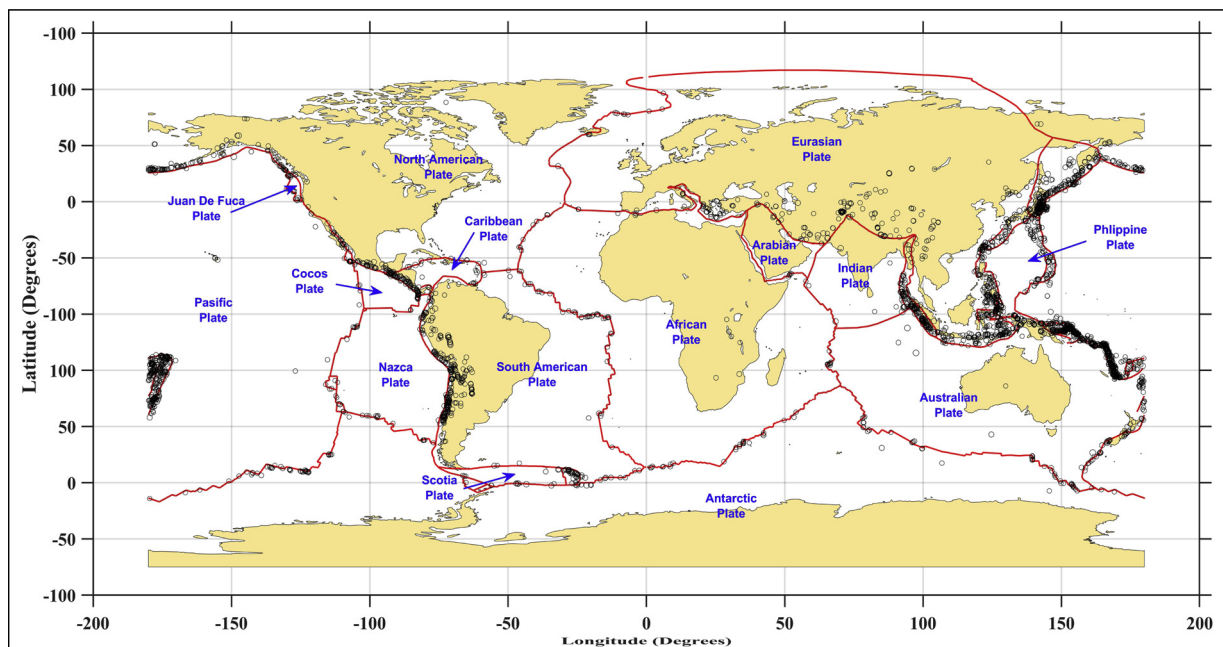


**Fig. 1.** Global epicenter distributions of 2942 earthquakes with  $M_w \geq 6$ . Red lines show the plate boundaries (created using MATLAB® 2017b) (For interpretation of the references to colour in this figure legend, the reader is referred to the web version of this article).

**Table 2**

The groups and numbers of earthquakes in which occurred between 2000 and 2019 according to their magnitudes.

Magnitude Groups	Number of Earthquakes	Number of Earthquakes Anomaly Detected
6.0 ≤ Mw < 6.5	2026	811
6.5 ≤ Mw < 7.0	622	273
7.0 ≤ Mw < 7.5	184	76
7.5 ≤ Mw < 8.0	87	33
8.0 ≤ Mw < 8.5	18	8
8.5 ≤ Mw < 9.0	3	1
9.0 ≤ Mw < 9.5	2	1

related to the studies made by Freund et al. (2009) and Freund (2011). Pulinets et al. (2015) explained that, the ionization before earthquake interact with the geophysical processes for the Lithosphere-Atmosphere-Ionosphere-Magnetosphere System in a number of physical and chemical process. The process in the appearance of ionospheric TEC anomalies due to earthquakes under the ocean can be related to physical mechanisms such as Ouzounov et al. (2011), detected possible earthquake precursors before the March 11, 2011 Tokyo earthquake which occurred under the ocean with infrared sensor data in satellites observing temperature changes in the earth's atmosphere. Pulinets and Davidenko (2018), investigated many earthquakes that occurred under the ocean and showed that radon release before earthquake increases the ionization level in the ionosphere. Pulinets et al. (2018), showed that radon activity before the earthquakes are related to Very Low Frequency (VLF), Electric Field (EF) and Acoustic Gravity Waves (AGW) in geochemical-thermal interface and in geochemical-electromagnetic interface and, they also yielded the schematic structure of these physical mechanisms by studying the earthquakes that occurred both on lands and under the ocean. In this context, ionospheric precursors of the earthquakes that occurred under the ocean can also be associated with the realization process of both geochemical-thermal and geochemical-electromagnetic physical mechanisms.

## 2.2. Obtaining TEC variations and space weather conditions data

In this study, global ionosphere maps including TEC (GIM-TEC) variations with time resolution in 2 h (two hours) and with a spatial resolution in 2.5 and 5 degrees in latitude and longitude provided by International GNSS Service (IGS) were used for the statistical analyses and therefore spatial variations of seismo-ionospheric disturbances of pre-earthquake ionospheric anomalies were investigated (Hernández-Pajares et al., 2009). We extracted the TEC data from Global Positioning System (GPS) ionex data during 2000–2019 years for global earthquakes of Mw ≥ 6.0 and investigated the seismo-ionospheric variations in TEC prior to the earthquake by using the TEC data of the grid points around the epicenter to interpolate the epicenter TEC data. TEC is expressed in TECU unit (TECU) where 1 TECU = 10<sup>16</sup>electron/m<sup>2</sup>.

Various effects such as solar activity, geomagnetic activity, human-induced effects or meteorological events are mainly affective on the ionospheric parameters (Aggarwal, 2015) especially in the Polar and Equatorial regions. The solar terrestrial conditions should be noticed to exclude anomalies that may have been caused by geomagnetic or solar activities when investigating the relationship between earthquake and ionospheric anomalies (Pulinets and Legen'ka, 2003). In addition, the ionosphere presents normal day-to-day, seasonal and diurnal changes making it difficult to describe possible pre-earthquake ionospheric anomalies as causes variations in the ionospheric parameters, such as GPS-TEC, on a regional scale (Afraimovich and Astafyeva, 2008). In order to distinguish the possible effects of earthquakes on the ionosphere layer from the sun and geomagnetic changes, detailed analysis for changes in space weather conditions requires index values (e.g., solar activity: Proton flux [Pf] at six different energy levels, Solar Flux

[F10.7], Extreme Ultraviolet [EUV<sub>01-50nm</sub>] and Extreme Ultraviolet [EUV<sub>26-34nm</sub>]; geomagnetic storm indices: Disturbance storm-time [Dst], Planetary Geomagnetic Activity Index [Kp], z component of Magnetic Field Index [Bz], Proton density [P<sub>d</sub>]) of different solar and geomagnetic space weather conditions. In most earthquake precursory studies Kp, Dst and F10.7 indices were used to eliminate the active space weather conditions (Cahyadi and Heki, 2013; Ho et al., 2013; Li et al., 2018; Shah and Jin, 2015; Zhao et al., 2010). In this study, thirteen different geomagnetic and solar index variations (i.e., Dst, Kp, Bz, P<sub>d</sub>, Pf with six threshold values, F10.7, EUV<sub>01-50nm</sub> and EUV<sub>26-34nm</sub>) were considered for space weather condition variations. We obtained the geomagnetic storm indices (Dst, Kp), magnetic field variations (Bz), solar activity indices (F10.7, EUV<sub>01-50nm</sub> and EUV<sub>26-34nm</sub>), proton density (P<sub>d</sub>) and proton flux variations with six different threshold values (Pfs) from Goddard Space Flight Center (GSFC) OMNI Web interface via <https://omniweb.gsfc.nasa.gov/form/dx1.html> and EUV Flux variations were obtained from the University of Southern California Space Sciences Center achieve from [http://www.usc.edu/dept/space\\_science/semdatafolder/semdownload.htm](http://www.usc.edu/dept/space_science/semdatafolder/semdownload.htm). The reason why we use this variety of solar and geomagnetic indices is to make more detailed analysis on anomalies that can be detected except earthquakes and to interpret the possible ionospheric anomalies due to earthquakes according to more accurate results.

## 2.3. Analysis of the GIM-TEC variations and space weather conditions

In this study, the data on F10.7 cm (Atıcı and Sağır, 2017; Bruevich et al., 2014; Vitinsky et al., 1986), EUV<sub>01-50nm</sub> and EUV<sub>26-34nm</sub> (Judge et al., 2011; Tsurutani et al., 2005), Kp (Astafyeva and Heki, 2011; Zolesi and Cander, 2014) and Dst (Contadakis et al., 2012; Hattori et al., 2011; Kamide et al., 1998), Bz (Dashora et al., 2009; Pulinets and Legen'ka, 2003), P<sub>d</sub> (King and Papitashvili, 2005) and Pfs (John and Kurian, 2009; Schwenn, 2004) changes were investigated according to the limit values, and quiet and active days which were not affected by space weather conditions were detected. As an example, September 12, 2006 La Rioja- Argentina earthquake (Mw = 6.0) was given in Figs. 2, 3 and 4.

As seen in Fig. 2, according to the limit values of geomagnetic storm indices, active days before the earthquake are due to the magnetic field (Bz = +5.5 nT) change in August 30, 2006; due to the magnetic field (Bz = -7.2 nT) and proton density (P<sub>d</sub> = 17.2 N<sub>p</sub>/cm<sup>3</sup>) changes which in August 31, 2006; due to the magnetic field (Bz = -5.7 nT) and geomagnetic storm (Kp = 4.3) changes in September 1, 2006; due to the magnetic field (Bz = -6.5 nT), proton density (P<sub>d</sub> = 18.4 N<sub>p</sub>/cm<sup>3</sup>) and geomagnetic storm (Kp = 5.7) changes in September 4, 2006. In Fig. 2, although Kp index cannot reach the limit value of 4.0 in August 31, the fact that Bz index changes (limit value = +5 nT) which is used as related to the earth magnetic field change and proton density change (limit value = 15N<sub>p</sub>/cm<sup>3</sup>) values exceed the limit values clearly show the necessity of the using more space weather condition index.

As seen in Fig. 3, although F10.7, the solar activity index, on September 8, 2006 is lower than the limit values of 150 sfu, the fact that the indices of EUV<sub>01-50nm</sub> and EUV<sub>26-34nm</sub> show the evidence actively which indicates the importance of using more indices of space weather conditions in the analysis. As seen in Figs. 3 and 4, according to the limit values of solar activity indices, active days before the earthquake are due to the excessive ultraviolet flux (EUV<sub>0.1-50nm</sub> = 1.29 × 10<sup>10</sup> cm<sup>2</sup>/s and EUV<sub>26-34nm</sub> = 2.48 × 10<sup>10</sup> cm<sup>2</sup>/s) changes which takes place on September 8, 2006; due to the excessive ultraviolet flux (EUV<sub>26-34nm</sub> = 2.47 × 10<sup>10</sup> cm<sup>2</sup>/s) and proton density (P<sub>d</sub> = 19.3 N<sub>p</sub>/cm<sup>3</sup>) changes that occurs on September 10, 2006. When the days of active space weather condition after the earthquake are examined, it can be clearly seen that active days are due to only the excessive ultraviolet flux (EUV<sub>0.1-50nm</sub> = 1.26 × 10<sup>10</sup> cm<sup>2</sup>/s and EUV<sub>26-34nm</sub> = 2.42 × 10<sup>10</sup> cm<sup>2</sup>/s) changes which takes place on September 13, 2006. By examining Figs. 2, 3 and 4 together, we detected quiet and active

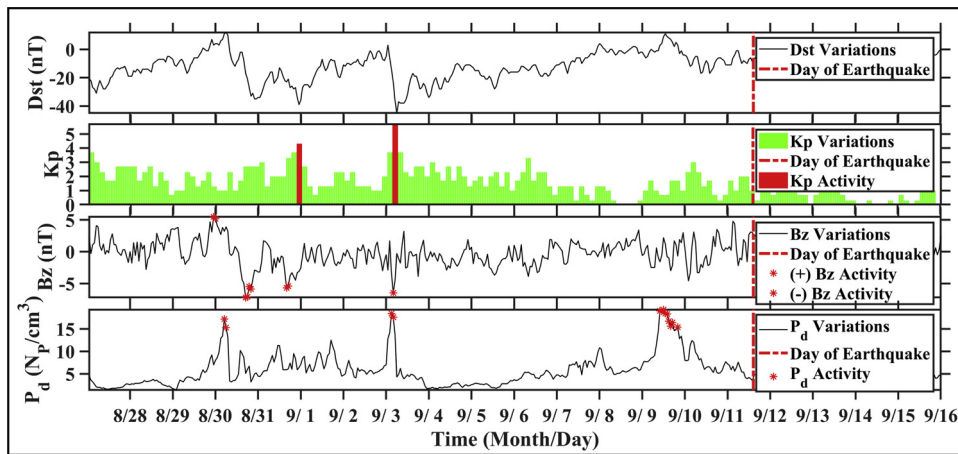


Fig. 2. Active days detected with geomagnetic storm indices (Disturbance storm-time [Dst], Planetary Geomagnetic Activity Index [Kp], z component of Magnetic Field Index [Bz], Proton density [ $P_d$ ]) for September 12, 2006 La Rioja, Argentina earthquake.

days according to all space weather conditions (Fig. 5). As shown in Fig. 5, when we analyse the space weather conditions before the earthquake in September 12, 2006 La Rioja-Argentina, earthquake day and the days of 1., 3., 5., 6., 7., 9., 10., 14. and 15., the days of 2., 3. and 4. before the earthquake were detected as quiet days, whereas the remaining days were considered as active days.

15-days moving median (MM) method is a quartile based statistical analysis technique and the investigation of seismo-ionospheric TEC anomalies can be done by using this application (Liu et al., 2009). Therefore, the MM values of GPS-TEC were firstly computed by using this method. In addition, we calculated the lower quartile (LQ) and upper quartile (UQ). The GPS-TEC values were assumed in the normal distribution the expected MM and LQ or UQ are  $m$  (mean) and  $\pm 1.34 \sigma$  (standard deviation) (Samuel et al., 2005). The lower bound [LB =  $MM - 1.5(MM - LQ)$ ] and upper bound [UB =  $MM + 1.5(UQ - MM)$ ] were estimated, respectively. Anomalies are identified when GPS-TEC variations are out of the range limited with the LB and UB (Liu et al., 2009). For instance, in order to generate MM, UB and LB for the 16th day, the TEC values for the first 15 days were utilized. Similarly, 15 days of TEC data between the 2nd and 16th day were used to generate bounds for the 17th day. If more than one-third of the data (e.g., eight hours are anomalous in a day) are greater or lesser than UBs and LBs in a day, this day was taken as anomalous (Liu et al., 2009; Ulukavak and Yalcinkaya, 2017a). For this work analyses for TEC changes obtained

from GIM-TEC maps of all earthquakes for 15-days before and 4-days after the main shock was prepared and ionospheric TEC changes in September 12, 2006 La Rioja-Argentina earthquake was given as the example (Fig. 6).

In this study, according to 15-days moving median statistical analysis method, day was accepted as possible earthquake precursor, in case the ratio of TEC anomaly numbers which takes place in the day of quiet space weather conditions to the total number of data in a day are greater than 4/12. The anomaly values calculated in Fig. 6 depict that some anomalies were observed before the earthquake occurrences such as 1–4 TECU positive anomaly on August 28, 2006; 0.3–1.8 TECU positive anomaly on September 1, 2006; 0.6 TECU positive anomaly on September 2, 2006; 0.4–3.3 TECU positive anomaly on September 4, 2006; 0.2–0.8 TECU positive anomaly on September 5, 2006; 0.3 TECU positive anomaly on September 6, 2006; 0.7 TECU positive anomaly on September 7, 2006; 0.8 TECU positive anomaly on September 8, 2006; 0.4 TECU positive anomaly on September 9, 2006; 2.9–4.5 TECU positive anomaly on September 10, 2006. On the other hand, the anomalies calculated after the earthquake, two anomaly changes can be seen as 3.4 TECU positive anomaly on September 13, 2006 and 0.2 TECU positive anomaly on September 15, 2006.

Both Figs. 5 and 6 shows that quiet (August 28, 2006, September 2 and 5, 2006) and active (September 1, 4, 8, 9 and 13, 2006) days on that the possible earthquake precursor occur were determined. In this

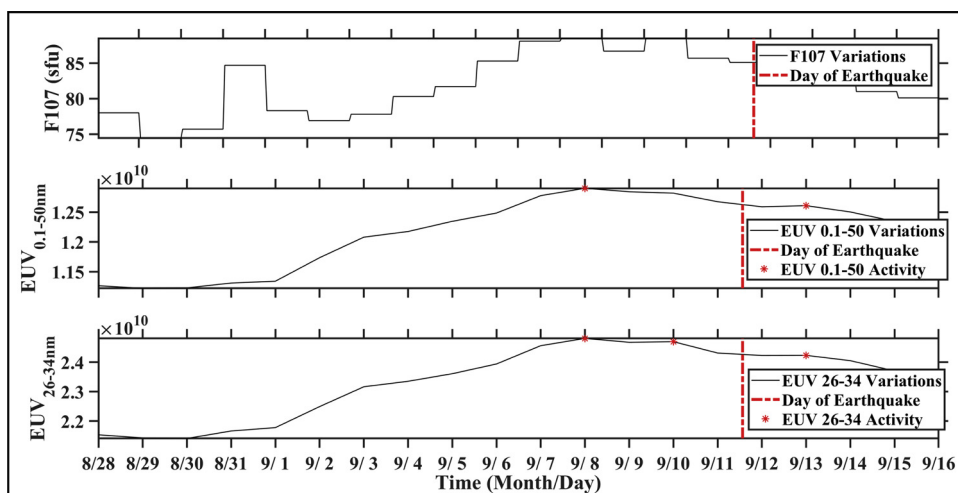


Fig. 3. Active days detected with solar activity indices (Solar Flux [F10.7], Extreme Ultraviolet [EUV<sub>0.1-50nm</sub>] and Extreme Ultraviolet [EUV<sub>26-34nm</sub>]) for September 12, 2006 La Rioja, Argentina earthquake.

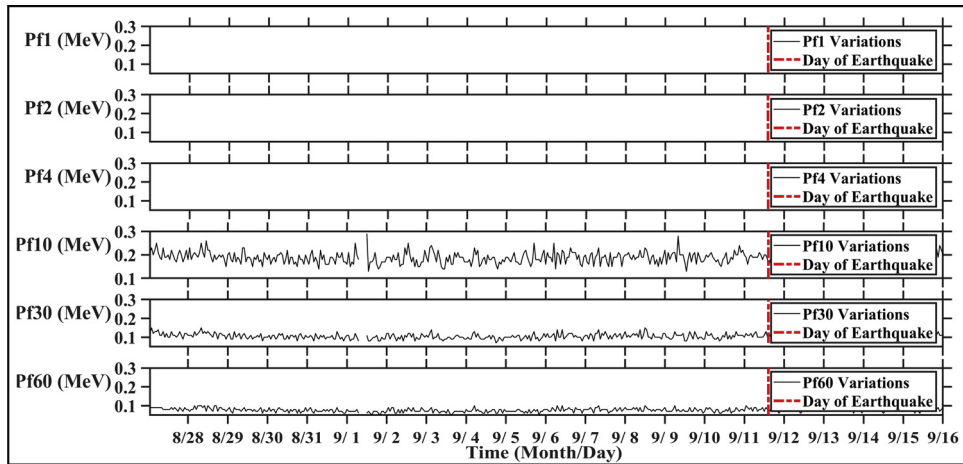


Fig. 4. Active days detected with solar activity indices (Proton flux [Pf] at six different energy levels) for September 12, 2006 La Rioja, Argentina earthquake.

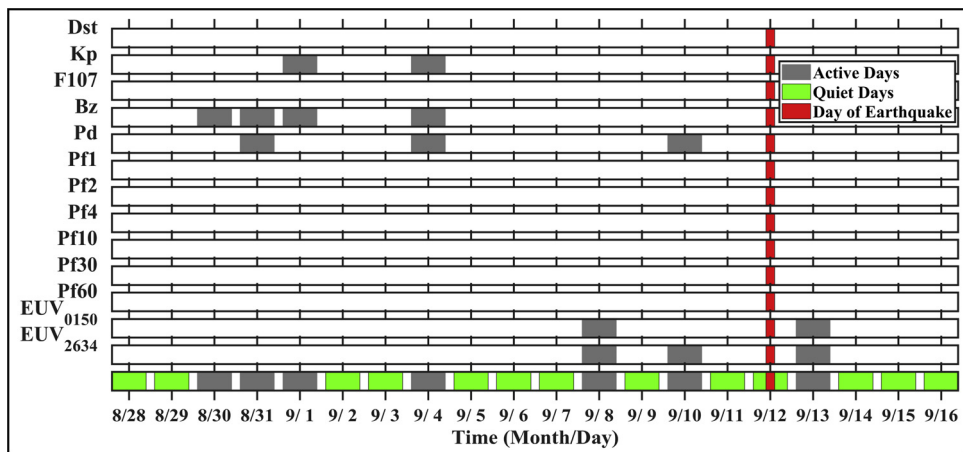


Fig. 5. A general representation of geomagnetic and solar activities.

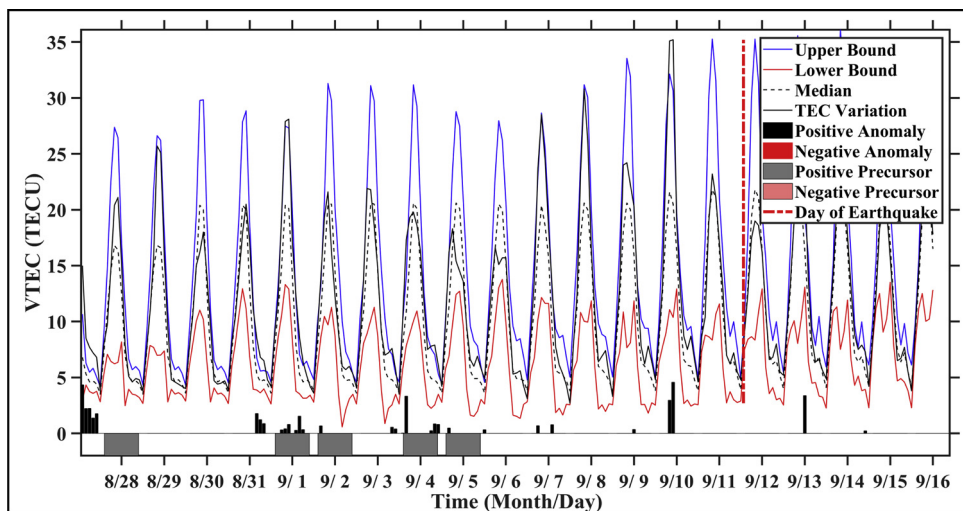


Fig. 6. Ionospheric TEC changes for September 12, 2006 La Rioja, Argentina earthquake.

context, positive ionospheric TEC precursors shown on the 7., 10. and 15. quiet days before the main shock can be considered as possible earthquake precursors since they occur in the quiet space weather conditions. Detailed analysis of active/quiet space weather conditions made for September 12, 2006 La Rioja-Argentina earthquake, detection of anomalies seen in ionospheric TEC changes and evaluation and

interpretation of these two analyses were achieved for 2942 global earthquakes.

### 3. Results and discussions

In the scope of this study, the quiet days were detected by analyzing

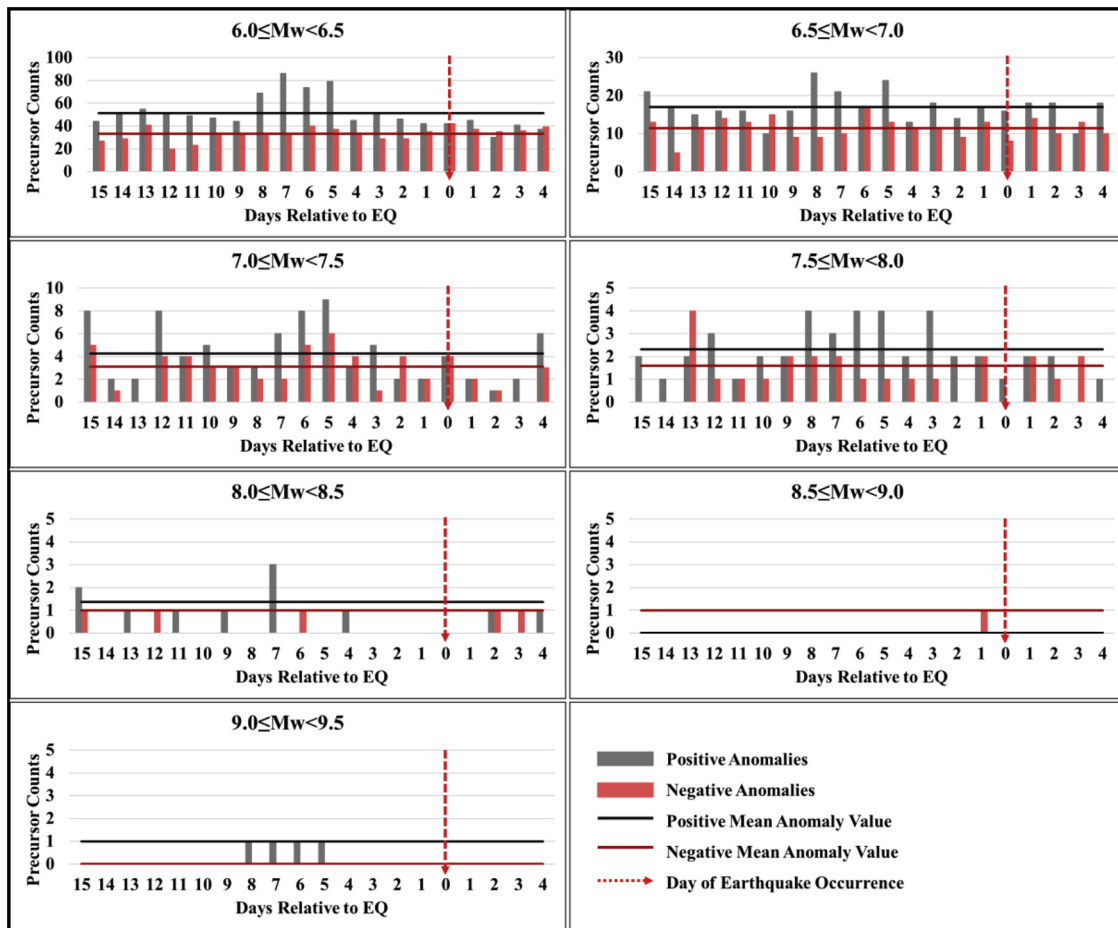


Fig. 7. Possible abnormal TEC days and earthquake numbers appeared in quiet days before the earthquakes of  $6.0 \leq Mw < 9.5$ .

the space weather condition indices according to Figs. 2, 3, 4 and 5 for 15-days before and 4-days after of all the earthquakes. Then, ionospheric TEC changes of earthquake epicenter obtained from GIM-TEC were analyzed by using 15-days moving median statistical analysis method and possible ionospheric TEC anomalies before the earthquake were determined (Fig. 6). Afterwards, by analyzing the results of space weather conditions and the anomalies obtained from ionospheric TEC changes together, possible ionospheric TEC precursors corresponding to quiet space weather conditions were identified. The earthquakes with anomalies, the numbers of positive and negative ionospheric TEC anomalies before and after the earthquakes obtained by grouping according to the earthquake magnitudes specified in Table 2 were calculated by adding according to days the anomalies were observed (Fig. 7). As seen Fig. 7, ionospheric TEC anomalies observed before the earthquake were detected at 5, 6, 7 and 8 days ago in the positive anomalies and 0, 5, 6 and 13 days ago in the negative anomalies for obtained the earthquakes of  $6.0 \leq Mw < 6.5$ ; at 5, 7, 8 and 15 days ago in the positive anomalies and 1, 5, 6 and 10 days ago in the negative anomalies for obtained the earthquakes of  $6.5 \leq Mw < 7.0$ ; at 5, 6, 12 and 15 days ago in the positive anomalies and 0, 2, 5, 6, 12 and 15 days ago in the negative anomalies for obtained the earthquakes of  $7.0 \leq Mw < 7.5$ ; at 3, 5, 6, 8 and 12 days ago in the positive anomalies and 1, 5, 7, 8, 9 and 13 days ago in the negative anomalies for obtained the earthquakes of  $7.5 \leq Mw < 8.0$ ; at 7 and 15 days ago in the positive anomalies and 6, 12 and 15 days ago in the negative anomalies for obtained the earthquakes of  $8.0 \leq Mw < 8.5$ . In addition, a negative anomaly was observed at 1 day ago for a single earthquake of  $8.5 \leq Mw < 9.0$  and a positive anomaly was detected at 5, 6, 7 and 8 days ago for a single earthquake of  $9.0 \leq Mw < 9.5$ . According to the results of study by Le et al. (2011), seismo-ionospheric anomalies closer to the

earthquake occurrence time (7 days ago) is obtained as the magnitude of earthquakes occurring at shallow depths ( $\leq 40\text{km}$ ) increases ( $M \geq 6$ ). The results of Le et al. (2011) confirm the statistical analysis of the present study (Fig. 7). In addition, when we looked at the results of study by Shah and Jin (2015), it is seen that seismo-ionospheric precursory anomaly of  $\sim 5$  days earlier detected for 1492 shallow ( $\leq 50\text{km}$ ) earthquakes with magnitude larger than 5.0 between 1998 and 2014 supports the occurrence range ( $\sim 5\text{--}8$ ) of seismo-ionospheric precursors obtained for the earthquakes of  $6.0 \leq Mw < 6.5$  in this study.

There are a lot of studies in the literature on this subject and many of them have investigated the possible ionospheric TEC changes which appeared prior to the earthquakes by using one or two earthquakes. The findings of these studies were generally performed to identify the possible ionospheric TEC precursors that preceded the earthquake (Afraimovich and Astafyeva, 2008; Aggarwal, 2015; Liu et al., 2011; Tariq et al., 2019; Zhu et al., 2013b). Previous literature studies show also that the anomalies that appeared prior to earthquakes with magnitude larger than 7.0 (Fuying et al., 2011; Tariq et al., 2019; Yao et al., 2012; Zhu et al., 2014, 2013b) compared to earthquakes with magnitude larger than 6.0 (Hattori et al., 2014; Kon et al., 2011; Liu et al., 2011; Şentürk and Çepni, 2018) moves away from the earthquake occurrence day. Jhuang et al. (2010) stated in their study that seismo-ionospheric anomalies of an earthquake with  $Mw = 8.0$  appear approximately 5–13 days ago before the earthquake.

A summary of several recent studies made in recent years on the detection of possible ionospheric TEC anomalies that occurred prior to the main shock was presented in Table 1. As seen in Table 1, the relationship between possible ionospheric TEC anomalies and earthquake was investigated before 1492 events at most. In addition, three different

indices (Dst, Kp, F10.7) values of space weather conditions were generally used in these researches and it was not clearly explained in these studies how many of the anomalies detected before the earthquakes occurrences were observed on quiet days in terms of space weather conditions. In this study, possible ionospheric TEC anomalies before 2942 earthquakes with magnitudes equal to and larger than 6 occurred between 2000–2019 were identified and, it was aimed to make an examination according to 13 different index values of space weather conditions (geomagnetic storm indices: Dst, Kp, Bz, P<sub>a</sub>; solar activity: F10.7, EUV<sub>01-50</sub> and EUV<sub>26-34</sub>, Pf at six different energy levels). For this purpose, quiet days were detected with more number of indexes of space weather conditions and the number of days before the main shocks that the possible ionospheric TEC anomalies occur was presented in a more reliable way. Also, the relationship between earthquake magnitudes and possible ionospheric TEC anomalies before the earthquakes was examined and discussed in this study. As a result of the analyses in the present study, positive and negative anomalies that appeared before the earthquakes were observed much earlier (~5-15 days ago) than the earthquake occurrence day (Fig. 7). These results reveal that a possible indicator of more stress and the energy that will emerge in the earthquake occurrence time will start to accumulate earlier (Rikitake 1987).

In the present study, the ratio of positive and negative anomaly numbers that appeared before the earthquake was calculated for different earthquake magnitude groups (Fig. 8). As seen in Fig. 8, changes in the groups of ionospheric TEC anomalies classified according to earthquake magnitudes can be given as follow: positive anomaly ratio for the earthquakes of  $6.0 \leq Mw < 6.5$  is 61 % and negative anomaly ratio is 39 %; 60 % positive anomaly ratio and 40 % negative anomaly ratio for the earthquakes of  $6.5 \leq Mw < 7.0$ ; 60 % positive anomaly ratio and 40 % negative anomaly ratio for the earthquakes of  $7.0 \leq Mw < 7.5$ ; 65 % positive anomaly ratio and 35 % negative anomaly ratio for the earthquakes of  $7.5 \leq Mw < 8.0$ ; 69 % positive anomaly ratio and 31 % negative anomaly ratio for the earthquakes of  $8.0 \leq Mw < 8.5$ . In addition, a negative anomaly ratio of 100 % for the earthquakes of  $8.5 \leq Mw < 9.0$  and a positive anomaly ratio of 100 % for the earthquakes of  $9.0 \leq Mw < 9.5$  were calculated because of single earthquake in these groups. The positive anomaly is generally calculated as larger than negative anomaly for different magnitude groups (Fig. 8).

Positive and negative mean ionospheric TEC anomaly values were calculated according to different earthquake magnitude groups and mean value of TEC anomaly changes determined in each group was calculated as 44 % TECU; positive anomaly for the earthquakes of  $6.0 \leq Mw < 6.5$  is 45.4 % TECU and negative anomaly is 42.8 % TECU; 45.8 % TECU positive anomaly and 40.5 % TECU negative anomaly for the earthquakes of  $6.5 \leq Mw < 7.0$ ; 47.3 % TECU positive anomaly and 42.7 % TECU negative anomaly for the earthquakes of  $7.0 \leq Mw < 7.5$ ; 42.1 % TECU positive anomaly and 41.8 % TECU negative anomaly for the earthquakes of  $7.5 \leq Mw < 8.0$ ; 40.0 % TECU positive anomaly and 38.9 % TECU negative anomaly for the earthquakes of  $8.0 \leq Mw < 8.5$ ; 41.7 % TECU negative anomaly for the earthquakes of  $8.5 \leq Mw < 9.0$ ; 54.2 % TECU positive anomaly for the earthquakes of  $9.0 \leq Mw < 9.5$  (Fig. 9).

#### 4. Conclusions

In this study, the effects of strong earthquakes occurring at different magnitudes on ionospheric TEC variations were examined. The relationships of GPS-TEC day-to-day changes to the magnitude of the earthquakes have been investigated. Although many researchers reported the existence of pre-earthquake ionospheric anomalies and discussed the possible origins, the coupling mechanisms among the lithosphere, atmosphere and ionosphere are still not fully understood. This study focuses only on the relationship between ionospheric TEC changes and different earthquake magnitudes before the main shock of

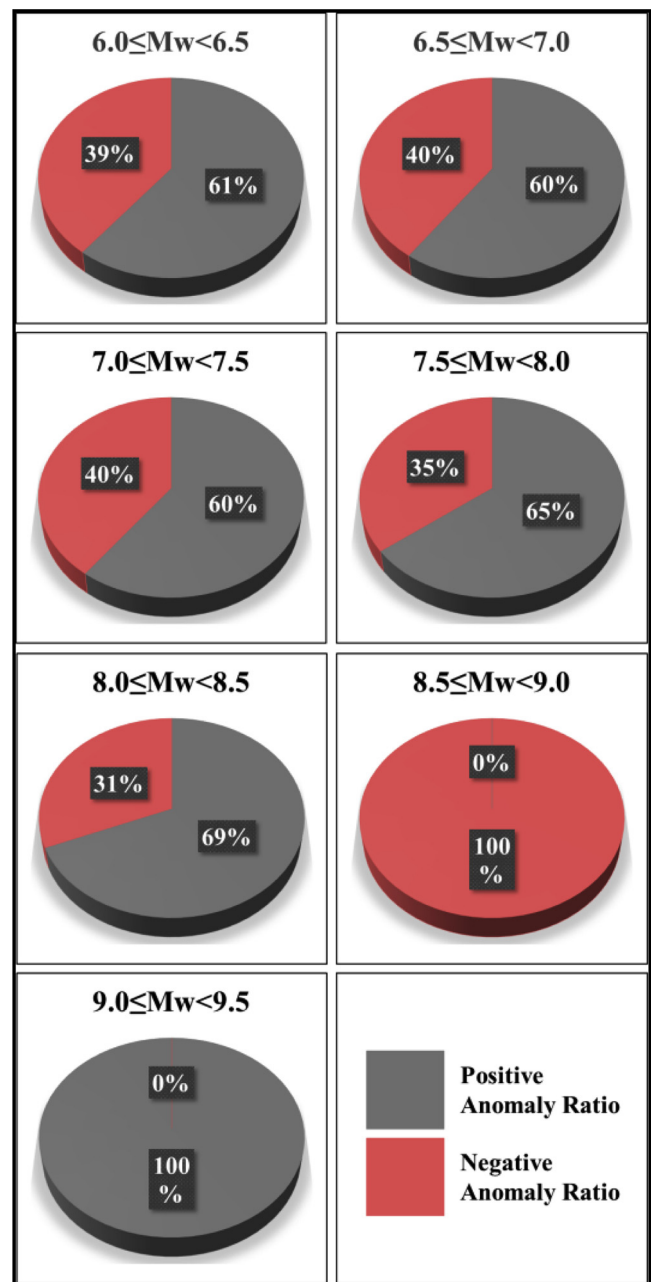


Fig. 8. Ratio of positive and negative anomaly numbers appeared in the quiet days before the earthquakes of  $6.0 \leq Mw < 9.5$ .

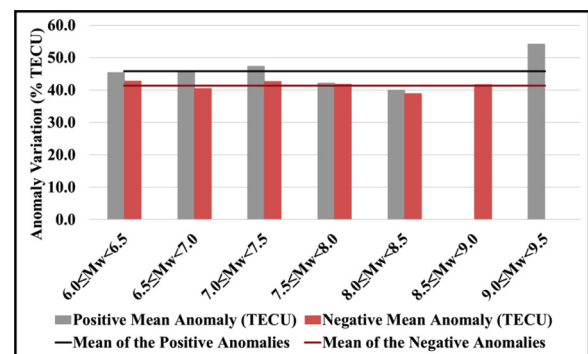


Fig. 9. Positive and negative mean anomaly variations.



seismic events.

In the scope of this study, an evaluation on the detection of precursors by using ionospheric TEC anomalies was achieved for different magnitude groups including 2942 earthquakes with magnitudes larger than and equal to 6.0 between 2000 and 2019. In this context, space weather condition indices (geomagnetic storm indices: Dst, Kp, Bz, P<sub>d</sub>; solar activity: F10.7, EUV<sub>01-50</sub> and EUV<sub>26-34</sub>, Pf at six different energy levels) more than 3 different indices (Dst, Kp, F10.7) commonly used in the literature were preferred in order to make more reliable detection of the quiet days with space weather conditions affecting ionospheric TEC anomalies.

Global earthquakes of  $6.0 \leq M_w < 9.5$  were considered for the statistical analysis and earthquakes were divided different magnitude groups with a 0.5 magnitude increment. Ionospheric TEC changes were taken from GIM-TEC maps and, positive and negative anomalies occurred in quiet space weather conditions in the day were identified by using for 15-days moving median statistical analysis method. It was accepted that as a possible earthquake precursor can be stated on that day if the ratio of the total number of anomalies observed to the total number of data in a day is larger than 4/12. In this way, precursory anomalies for each magnitude group were observed in approximately 5–13, ~5-10, ~5-15, ~3-13, ~7-15, ~1 and ~5-8 days ago for the earthquakes of  $6.0 \leq M_w < 6.5$ ,  $6.5 \leq M_w < 7.0$ ,  $7.0 \leq M_w < 7.5$ ,  $7.5 \leq M_w < 8.0$ ,  $8.0 \leq M_w < 8.5$ ,  $8.5 \leq M_w < 9.0$ , and  $9.0 \leq M_w < 9.5$ , respectively. Thus, we observed that ionospheric TEC anomalies were detected with earthquake precursor in earlier day from the earthquake as the earthquake magnitudes increases. However, changes of the mean TEC anomaly value were calculated as 44.2 % TECU for different magnitude groups and it was identified that the numbers of positive anomaly in each group are more than the numbers of negative anomaly. Consequently, the results of this study can finally contribute to the earthquake prediction in the short term providing an empirical and a proven statistical technique to the literature.

#### Declaration of Competing Interest

The authors declare that they have no known competing financial interests or personal relationships that could have appeared to influence the work reported in this paper.

#### Acknowledgements

The authors would like to thank, the CDDIS (Crustal Dynamics Data and Information System) data and products archive, for providing the IONEX files, and also, we acknowledge the use of NASA/GSFC's Space Physics Data Facility's OMNIWeb (or CDAWeb or FTP) service, and OMNI data. We would like to express our special thanks to TUBITAK (The Scientific and Technological Research Council of Turkey), Environment, Atmosphere, Earth and Marine Science Research Support Group (CAYDAG) that supporting our project with grant no. 116Y109.

#### Appendix A. Supplementary data

Supplementary material related to this article can be found, in the online version, at doi:<https://doi.org/10.1016/j.jog.2020.101721>.

#### References

Afraimovich, E.L., Astafyeva, E.I., 2008. TEC anomalies - Local TEC changes prior to earthquakes or TEC response to solar and geomagnetic activity changes? *Earth Planets Sp.* 60, 961–966. <https://doi.org/10.1186/BF03352851>.

Aggarwal, M., 2015. Anomalous changes in ionospheric TEC during an earthquake event of 13-14 April 2010 in the Chinese sector. *Adv. Space Res.* 56, 1400–1412. <https://doi.org/10.1016/j.asr.2015.07.007>.

Astafyeva, E., Heki, K., 2011. Vertical TEC over seismically active region during low solar activity. *J. Atmos Solar-Terrestrial Phys.* 73, 1643–1652. <https://doi.org/10.1016/j.jastp.2011.02.020>.

Atci, R., Sağır, S., 2017. The investigation of relationship between solar parameters and

total Electron content over mid-latitude ionosphere. *Celal Bayar. Univ. J. Sci.* 13, 707–716. <https://doi.org/10.18466/cbayarfb.339346>.

Bruevich, E.A., Bruevich, V.V., Yakunina, G.V., 2014. Changed relation between solar 10.7-cm radio flux and some activity indices which describe the radiation at different altitudes of atmosphere during cycles 21-23. *J. Astrophys. Astron.* 35, 1–15. <https://doi.org/10.1007/s12036-014-9258-0>.

Cahyadi, M.N., Heki, K., 2013. Ionospheric disturbances of the 2007 Bengkulu and the 2005 Nias earthquakes, Sumatra, observed with a regional GPS network. *J. Geophys. Res. Sp. Phys.* 118, 1777–1787. <https://doi.org/10.1002/jgra.50208>.

Contadakis, M.E., Arabelos, D.N., Pikridas, C., Spatalas, S.D., 2012. Total electron content variations over southern Europe before and during the M 6.3 Abruzzo earthquake of April 6, 2009. *Ann. Geophys.* 55, 83–93. <https://doi.org/10.4401/ag-5322>.

Dashora, N., Sharma, S., Dabas, R.S., Alex, S., Pandey, R., 2009. Large enhancements in low latitude total electron content during 15 May 2005 geomagnetic storm in Indian zone. *Ann. Geophys.* 27, 1803–1820. <https://doi.org/10.5194/angeo-27-1803-2009>.

Fidani, C., 2010. The earthquake lights (EQL) of the 6 April 2009 Aquila earthquake, in Central Italy. *Nat. Hazards Earth Syst. Sci.* 10, 967–978. <https://doi.org/10.5194/nhess-10-967-2010>.

Freund, F., 2011. Pre-earthquake signals: underlying physical processes. *J. Asian Earth Sci.* 41, 383–400. <https://doi.org/10.1016/j.jseas.2010.03.009>.

Freund, F.T., Kulahci, I.G., Cyr, G., Ling, J., Winnick, M., Tregloan-Reed, J., Freund, M.M., 2009. Air ionization at rock surfaces and pre-earthquake signals. *J. Atmos Solar-Terrestrial Phys.* 71, 1824–1834. <https://doi.org/10.1016/j.jastp.2009.07.013>.

Fuying, Z., Yun, W., Yiyan, Z., Jian, L., 2011. A statistical investigation of pre-earthquake ionospheric TEC anomalies. *Geod Geodyn* 2, 61–65. <https://doi.org/10.3724/sp.j.1246.2011.00061>.

Geller, R.J., 2007. Earthquake prediction: a critical review. *Geophys J. Int.* 131, 425–450. <https://doi.org/10.1111/j.1365-246x.1997.tb06588.x>.

Guo, G., Wang, B., 2008. Cloud anomaly before Iran earthquake. *Int. J. Remote Sens.* 29, 1921–1928. <https://doi.org/10.1080/01431160701373762>.

Hattori, K., Kon, S., Nishihashi, M., 2011. Ionospheric anomalies possibly associated with M ≥ 6 earthquakes in Japan during 1998–2011: case studies and statistical study. 2011 30th URSI General Assembly and Scientific Symposium. <https://doi.org/10.1109/URSIGASS.2011.6051011>. URSIGASS 2011.

Hattori, K., Hirooka, S., Kunimitsu, M., Ichikawa, T., Han, P., 2014. Ionospheric Anomaly As an Earthquake Precursor: Case and Statistical Studies During 1998–2012 Around Japan. <https://doi.org/10.1109/ursigass.2014.6929866>.

He, L., Heki, K., 2017. Ionospheric anomalies immediately before Mw7.0–8.0 earthquakes. *J. Geophys. Res. Sp. Phys.* 122, 8659–8678. <https://doi.org/10.1002/2017JA024012>.

Heki, K., 2011. Ionospheric electron enhancement preceding the 2011 Tohoku-Oki earthquake. *Geophys. Res. Lett.* 38, 1–5. <https://doi.org/10.1029/2011GL047908>.

Hernández-Pajares, M., Juan, J.M., Sanz, J., Orus, R., Garcia-Rigo, A., Felzens, J., Komjathy, A., Schaer, S.C., Krankowski, A., 2009. The IGS VTEC maps: a reliable source of ionospheric information since 1998. *J. Geod.* 83, 263–275. <https://doi.org/10.1007/s00190-008-0266-1>.

Ho, Y.Y., Jhuang, H.K., Su, Y.C., Liu, J.Y., 2013. Seismo-ionospheric anomalies in total electron content of the GIM and electron density of DEMETER before the 27 February 2010 M8.8 Chile earthquake. *Adv. Sp. Res.* 51, 2309–2315. <https://doi.org/10.1016/j.asr.2013.02.006>.

Holliday, J.R., Nanjo, K.Z., Tiampo, K.F., Rundle, J.B., Turcotte, D.L., 2005. Earthquake forecasting and its verification. *Nonlinear Process. Geophys.* 12, 965–977. <https://doi.org/10.5194/npg-12-965-2005>.

Huang, Q., Sobolev, G.A., Nagao, T., 2001. Characteristics of the seismic quiescence and activation patterns before the M = 7.2 Kobe earthquake, January 17, 1995. *Tectonophysics* 337, 99–116. [https://doi.org/10.1016/S0040-1951\(01\)00073-7](https://doi.org/10.1016/S0040-1951(01)00073-7).

Huang, F., Li, M., Ma, Y., Han, Y., Tian, L., Yan, W., Li, X., 2017. Studies on earthquake precursors in China: a review for recent 50 years. *Geod Geodyn.* <https://doi.org/10.1016/j.jog.2016.12.002>.

Jhuang, H.K., Ho, Y.Y., Kakinami, Y., Liu, J.Y., Oyama, K.I., Parrot, M., Hattori, K., Nishihashi, M., Zhang, D., 2010. Seismo-ionospheric anomalies of the GPS-TEC appear before the 12 May 2008 magnitude 8.0 Wenchuan Earthquake. *Int. J. Remote Sens.* 31, 3579–3587. <https://doi.org/10.1080/01431161003727796>.

John, S., Kurian, P.J., 2009. A statistical study of the interdependence of solar wind parameters. *Res. Astron. Astrophys.* 9, 485–493. <https://doi.org/10.1088/1674-4527/9/4/011>.

Judge, D.L., McMullin, D.R., Ogawa, H.S., Hovestadt, D., Klecker, B., Hilchenbach, M., Möbius, E., Canfield, L.R., Vest, R.E., Watts, R., Tarrío, C., Kühne, M., Wurz, P., 2011. First solar EUV irradiances obtained from SOHO by the CELIAS/SEM. *Solar Electromagnetic Radiation Study for Solar Cycle 22*. pp. 161–173. [https://doi.org/10.1007/978-94-011-5000-2\\_12](https://doi.org/10.1007/978-94-011-5000-2_12).

Kamide, Y., Yokoyama, N., Gonzalez, W., Tsurutani, B.T., Daglis, I.A., Brekke, A., Masuda, S., 1998. Two-step development of geomagnetic storms. *J. Geophys. Res. Phys.* 103, 6917–6921. <https://doi.org/10.1029/97ja03337>.

King, J.H., Papitashvili, N.E., 2005. Solar wind spatial scales in and comparisons of hourly Wind and ACE plasma and magnetic field data. *J. Geophys. Res. Sp. Phys.* 110, 1–8. <https://doi.org/10.1029/2004JA010649>.

Kon, S., Nishihashi, M., Hattori, K., 2011. Ionospheric anomalies possibly associated with M 6.0 earthquakes in the Japan area during 1998–2010: Case studies and statistical study. *J. Asian Earth Sci.* 41, 410–420. <https://doi.org/10.1016/j.jseas.2010.10.005>.

Kuo, C.L., Huba, J.D., Joyce, G., Lee, L.C., 2011. Ionosphere plasma bubbles and density variations induced by pre-earthquake rock currents and associated surface charges. *J. Geophys. Res. Sp. Phys.* 116. <https://doi.org/10.1029/2011JA016628>.

Le, H., Liu, J.Y., Liu, L., 2011. A statistical analysis of ionospheric anomalies before 736 M6.0+ earthquakes during 2002–2010. *J. Geophys. Res. Sp. Phys.* 116, 1–5. <https://doi.org/10.1029/2011JA016628>.

- [doi.org/10.1029/2010JA015781](https://doi.org/10.1029/2010JA015781).
- Li, M., Parrot, M., 2013. Statistical analysis of an ionospheric parameter as a base for earthquake prediction. *J. Geophys. Res. Sp. Phys.* 118, 3731–3739. <https://doi.org/10.1002/jgra.50313>.
- Li, W., Yue, J., Guo, J., Yang, Y., Zou, B., Shen, Y., Zhang, K., 2018. Statistical seismo-ionospheric precursors of M7.0+ earthquakes in Circum-Pacific seismic belt by GPS TEC measurements. *Adv. Space Res.* 61, 1206–1219. <https://doi.org/10.1016/j.asr.2017.12.013>.
- Liu, J.Y., Chuo, Y.J., Shan, S.J., Tsai, Y.B., Chen, Y.I., Pulinet, S.A., Yu, S.B., 2004. Pre-earthquake ionospheric anomalies registered by continuous GPS TEC measurements. *Ann. Geophys.* <https://doi.org/10.5194/angeo-22-1585-2004>.
- Liu, J.Y., Chen, Y.I., Chuo, Y.J., Chen, C.S., 2006. A statistical investigation of pre-earthquake ionospheric anomaly. *J. Geophys. Res. Sp. Phys.* <https://doi.org/10.1029/2005JA011333>.
- Liu, J.Y., Chen, Y.I., Chen, C.H., Liu, C.Y., Chen, C.Y., Nishihashi, M., Li, J.Z., Xia, Y.Q., Oyama, K.I., Hattori, K., Lin, C.H., 2009. Seismoionospheric GPS total electron content anomalies observed. Before the 12 May 2008 Mw7.9 Wenchuan earthquake. *J. Geophys. Res. Sp. Phys.* 114, 1–10. <https://doi.org/10.1029/2008JA013698>.
- Liu, C.Y., Liu, J.Y., Chen, W.S., Li, J.Z., Xia, Y.Q., Cui, X.Y., 2011. An integrated study of anomalies observed before four major earthquakes: 2004 Sumatra M9.3, 2006 Pingtung M7.0, 2007 Chuetsu Oki M6.8, and 2008 Wenchuan M8.0. *J. Asian Earth Sci.* 41, 401–409. <https://doi.org/10.1016/j.jseaeas.2010.05.012>.
- Namgaladze, A.A., Klimenko, M.V., Klimenko, V.V., Zakharenkova, I.E., 2009. Physical mechanism and mathematical modeling of earthquake ionospheric precursors registered in total electron content. *Geomagn. Aeron.* 49, 252–262. <https://doi.org/10.1134/s0016793209020169>.
- Nanjo, K.Z., Holliday, J.R., Chen, C., Rundle, J.B., Turcotte, D.L., 2006. Application of a modified pattern informatics method to forecasting the locations of future large earthquakes in the central Japan. *Tectonophysics* 424, 351–366. <https://doi.org/10.1016/j.tecto.2006.03.043>.
- Ouzounov, D., Pulinet, S., Romanov, Alexey, Romanov, Alexander, Tsybulya, K., Davidenko, D., Kafatos, M., Taylor, P., 2011. Atmosphere-ionosphere response to the M9 Tohoku earthquake revealed by multi-instrument space-borne and ground observations: Preliminary results. *Earth Sci.* 24, 557–564. <https://doi.org/10.1007/s11589-011-0817-z>.
- Öztürk, S., 2011. Characteristics of seismic activity in the western, central and eastern parts of the North Anatolian Fault Zone, Turkey: temporal and spatial analysis. *Acta Geophys.* 59, 209–238. <https://doi.org/10.2478/s11600-010-0050-5>.
- Pulinet, S.A., 1998. Strong earthquake prediction possibility with the help of topside sounding from satellites. *Adv. Space Res.* 21, 455–458. [https://doi.org/10.1016/S0273-1177\(97\)00880-6](https://doi.org/10.1016/S0273-1177(97)00880-6).
- Pulinet, S.A., Davidenko, D.V., 2018. The Nocturnal Positive Ionospheric Anomaly of Electron Density as a Short-Term Earthquake Precursor and the Possible Physical Mechanism of Its Formation. *Geomagn. Aeron.* 58, 559–570. <https://doi.org/10.1134/S0016793218040126>.
- Pulinet, S.A., Legen'ka, A.D., 2003. Spatial-temporal characteristics of large scale disturbances of electron density observed in the ionospheric F-region before strong earthquakes. *Cosm. Res.* 41, 221–229. <https://doi.org/10.1023/A:1024046814173>.
- Pulinet, S.A., Ouzounov, D., Karelin, A.V., Boyarchuk, K.A., Pokhmelnikh, L.A., 2006. The physical nature of thermal anomalies observed before strong earthquakes. *Phys. Chem. Earth* 31, 143–153. <https://doi.org/10.1016/j.pce.2006.02.042>.
- Pulinet, S.A., Ouzounov, D.P., Karelin, A.V., Davidenko, D.V., 2015. Physical bases of the generation of short-term earthquake precursors: a complex model of ionization-induced geophysical processes in the lithosphere-atmosphere-ionosphere-magnetosphere system. *Geomagn. Aeron.* 55, 521–538. <https://doi.org/10.1134/S0016793215040131>.
- Pulinet, S., Ouzounov, D., Karelin, A., Davidenko, D., 2018. Lithosphere-Atmosphere-Ionosphere-Magnetosphere Coupling-A Concept for Pre-Earthquake Signals Generation. pp. 77–98. <https://doi.org/10.1002/9781119156949.ch6>.
- Rundle, J.B., Turcotte, D.L., Shcherbakov, R., Klein, W., Sammis, C., 2003. Statistical physics approach to understanding the multiscale dynamics of earthquake fault systems. *Rev. Geophys.* 41, 1–30. <https://doi.org/10.1029/2003RG000135>.
- Samuel, K., Balakrishnan, N., Read, C.B., Vidakovic, B., 2005. *Encyclopedia of Statistical Sciences*. John Wiley and Sons, New Jersey.
- Schwenn, R., 2004. Solar Wind: Global Properties, in: *The Encyclopedia of Astronomy and Astrophysics*. Institute of Physics Publishing Ltd, Bristol. <https://doi.org/10.1888/0333750888/2301>.
- Şentürk, E., Çepni, M.S., 2018. A statistical analysis of seismo-ionospheric TEC anomalies before 63 M w  $\geq$  5.0 earthquakes in Turkey during 2003–2016. *Acta Geophys.* 66, 1495–1507. <https://doi.org/10.1007/s11600-018-0214-2>.
- Shah, M., Jin, S., 2015. Statistical characteristics of seismo-ionospheric GPS TEC disturbances prior to global Mw  $\geq$  5.0 earthquakes (1998–2014). *J. Geodyn.* 92, 42–49. <https://doi.org/10.1016/j.jog.2015.10.002>.
- Shcherbakov, R., 2003. Nonlinear dynamics of the lithosphere and earthquake prediction. *Eos, Transactions American Geophysical Union*, 1st ed. Springer-Verlag Berlin Heidelberg, New York. <https://doi.org/10.1029/2003eo330008>.
- Sobolev, G.A., Tyupkin, Y.S., 1997. Low-seismicity precursors of large earthquakes in Kamchatka. *Volcanol Seismol.* 18, 433–446.
- St-Laurent, F., Derr, J.S., Freund, F.T., 2006. Earthquake lights and the stress-activation of positive hole charge carriers in rocks. *Phys. Chem. Earth* 31, 305–312. <https://doi.org/10.1016/j.pce.2006.02.003>.
- Sunardi, B., Muslim, B., Sakya, A.E., Rohadi, S., Sulastri, S., Murjaya, J., 2018. Ionospheric earthquake effects detection based on total electron content (TEC) GPS correlation. *IOP Conference Series: Earth and Environmental Science*. <https://doi.org/10.1088/1755-1315/132/1/012014>.
- Sykes, L.R., 2002. Intermediate- and long-term earthquake prediction. *Proc. Natl. Acad. Sci.* 93, 3732–3739. <https://doi.org/10.1073/pnas.93.9.3732>.
- Tao, D., Cao, J., Battiston, R., Li, L., Ma, Y., Liu, W., Zhima, Z., Wang, L., Wray Dunlop, M., 2017. Seismo-ionospheric anomalies in ionospheric TEC and plasma density before the 17 July 2006 M7.7 south of Java earthquake. *Ann. Geophys.* 35, 589–598. <https://doi.org/10.5194/angeo-35-589-2017>.
- Tariq, M.A., Shah, M., Hernández-Pajares, M., Iqbal, T., 2019. Pre-earthquake ionospheric anomalies before three major earthquakes by GPS-TEC and GIM-TEC data during 2015–2017. *Adv. Space Res.* <https://doi.org/10.1016/j.asr.2018.12.028>.
- Thomas, J.N., Huard, J., Masci, F., 2017. A statistical study of global ionospheric map total electron content changes prior to occurrences of M  $\geq$  6.0 earthquakes during 2000–2014. *J. Geophys. Res. Sp. Phys.* 122, 2151–2161. <https://doi.org/10.1002/2016JA023652>.
- Tiampo, K.F., Rundle, J.B., McGinnis, S.A., Klein, W., 2002. Pattern dynamics and forecast methods in seismically active regions. *Pure Appl. Geophys.* 159, 2429–2467. <https://doi.org/10.1007/s00024-002-8742-7>.
- Tronin, A.A., Biagi, P.F., Molchanov, O.A., Khatkevich, Y.M., Gordeev, E.I., 2004. Temperature variations related to earthquakes from simultaneous observation at the ground stations and by satellites in Kamchatka area. *Phys. Chem. Earth* 29, 501–506. <https://doi.org/10.1016/j.pce.2003.09.024>.
- Tsurutani, B.T., Judge, D.L., Guarneri, F.L., Gangopadhyay, P., Jones, A.R., Nuttall, J., Zambon, G.A., Didkovsky, L., Mannucci, A.J., Iijima, B., Meier, R.R., Immel, T.J., Woods, T.N., Prasad, S., Floyd, L., Huba, J., Solomon, S.C., Straus, P., Viereck, R., 2005. The October 28, 2003 extreme EUV solar flare and resultant extreme ionospheric effects: comparison to other Halloween events and the Bastille Day event. *Geophys. Res. Lett.* 32, 1–4. <https://doi.org/10.1029/2004GL021475>.
- Ulukavak, M., Yalcinkaya, M., 2017a. Precursor analysis of ionospheric GPS-TEC variations before the 2010 M7.2 Baja California earthquake. *Geomatics. Nat. Hazards Risk* 8, 295–308. <https://doi.org/10.1080/19475705.2016.1208684>.
- Ulukavak, M., Yalcinkaya, M., 2017b. INVESTIGATION OF THE RELATIONSHIP BETWEEN IONOSPHERIC TEC ANOMALY VARIATIONS AND FAULT TYPES BEFORE THE EARTHQUAKES, in: *ISPRS annals of the photogrammetry, Remote Sensing and Spatial Information Sciences*. <https://doi.org/10.5194/isprs-annals-IV-4-W4-383-2017>.
- Varotsos, P., Alexopoulos, K., 1984. Physical properties of the variations of the electric field of the earth preceding earthquakes. II. determination of epicenter and magnitude. *Tectonophysics* 110, 99–125. [https://doi.org/10.1016/0040-1951\(84\)90060-X](https://doi.org/10.1016/0040-1951(84)90060-X).
- Vitinsky, Y.I., Kopecky, M., Kuklin, G.V., 1986. *The Statistics of Sunspot-formation Activity*. Izdatel'stvo Nauka, Moscow.
- Wiemer, S., 2011. A software package to analyze seismicity: ZMAP. *Seismol. Res. Lett.* 72, 373–382. <https://doi.org/10.1785/gssrl.72.3.373>.
- Xia, C., Wang, Q., Yu, T., Xu, G., Yang, S., 2011. Variations of ionospheric total electron content before three strong earthquakes in the Qinghai-Tibet region. *Adv. Space Res.* 47, 506–514. <https://doi.org/10.1016/j.asr.2010.09.006>.
- Yao, Y.B., Chen, P., Zhang, S., Chen, J.J., Yan, F., Peng, W.F., 2012. Analysis of pre-earthquake ionospheric anomalies before the global M = 7.0+ earthquakes in 2010. *Nat. Hazards Earth Syst. Sci.* <https://doi.org/10.5194/nhess-12-575-2012>.
- Zhao, B.Q., Wang, M., Yu, T., Xu, G.R., Wan, W.X., Liu, L.B., 2010. Ionospheric total electron content variations prior to the 2008 Wenchuan Earthquake. *Int. J. Remote Sens.* 31, 3545–3557. <https://doi.org/10.1080/01431161003727622>.
- Zhu, F., Wu, Y., Zhou, Y., Gao, Y., 2013a. Temporal and spatial distribution of GPS-TEC anomalies prior to the strong earthquakes. *Astrophys. Space Sci.* 345, 239–246. <https://doi.org/10.1007/s10509-013-1411-8>.
- Zhu, F., Zhou, Y., Wu, Y., 2013b. Anomalous variation in GPS TEC prior to the 11 April 2012 Sumatra earthquake. *Astrophys. Space Sci.* 345, 231–237. <https://doi.org/10.1007/s10509-013-1389-2>.
- Zhu, F., Zhou, Y., Lin, J., Su, F., 2014. A statistical study on the temporal distribution of ionospheric TEC anomalies prior to M7.0+ earthquakes during 2003–2012. *Astrophys. Space Sci.* 350, 449–457. <https://doi.org/10.1007/s10509-014-1777-2>.
- Zhu, F., Lin, J., Su, F., Zhou, Y., 2016. A spatial analysis of the ionospheric TEC anomalies prior to M7.0+ earthquakes during 2003–2014. *Adv. Space Res.* 58, 1732–1738. <https://doi.org/10.1016/j.asr.2016.06.040>.
- Zhu, F., Su, F., Lin, J., 2018. Statistical analysis of TEC anomalies prior to M6.0+ earthquakes during 2003–2014. *Pure Appl. Geophys.* 175, 3441–3450. <https://doi.org/10.1007/s00024-018-1869-y>.
- Zolesi, B., Cander, L.R., 2014. *Ionospheric prediction and forecasting*. Ionospheric Prediction and Forecasting, 1st ed. Springer-Verlag, Berlin Heidelberg, London. <https://doi.org/10.1007/978-3-642-38430-1>.